

CGRO/OSSE observations of the Cassiopeia A SNR

L.-S. The¹, M. D. Leising¹, J. D. Kurfess², W. N. Johnson², D. H. Hartmann¹, N. Gehrels³, J. E. Grove², and W. R. Purcell⁴

¹ Department of Physics & Astronomy, Clemson University, Clemson, SC 29634-1911, USA

² E.O. Hulburt Center for Space Research, Naval Research Laboratory, Code 7650, Washington, DC 20375-5320, USA

³ NASA/Goddard Space Flight Center, Mail Code 661, Greenbelt, MD 20771, USA

⁴ Department of Physics & Astronomy, Northwestern University, Evanston, IL 60208, USA

Received October 1, 1995; accepted , 1995

Abstract. We present all OSSE observations to date of the Cas A supernova remnant. The objectives are to detect the ⁴⁴Ti lines, one of which has been reportedly detected by COMPTEL, and the hard X-ray continuum above 40 keV, as indicated by HEAO-A2 measurements. Our best fit flux in each of three ⁴⁴Ti lines is $(+1.76 \pm_{1.48}^{1.51}) \times 10^{-5} \gamma \text{ cm}^{-2} \text{ s}^{-1}$ with $\chi^2_\nu = 1.01$, d.o.f.=1780. The implied ⁴⁴Ti mass of $\sim 10^{-4} M_\odot$ is compatible with explosive nucleosynthesis calculations. OSSE detected also a continuum below 200 keV at better than 4σ confidence level with a flux of $\sim 9 \times 10^{-4} \gamma \text{ cm}^{-2} \text{ s}^{-1} \text{ MeV}^{-1}$ at 100 keV. This continuum can be fitted equally well with a power law, an exponential, or a thermal bremsstrahlung model. The implied temperature of $kT \approx 35 \text{ keV}$ can be interpreted as the emission from the shocked circumstellar matter (CSM) by the primary blastwave of the supernova. Alternatively, the continuum can also be interpreted as bremsstrahlung from accelerated electrons that are also producing the observed radio emission.

Key words: gamma rays: observations – ISM: individual objects: Cassiopeia A SNR – Nuclear reactions, nucleosynthesis, abundances

1. Introduction

Gamma-ray observations of Cas A have generated some excitement since the 4σ detection of the 1.157 MeV ⁴⁴Ti line by COMPTEL on CGRO (Iyudin 1994). Its importance to nuclear astrophysics is that the ejected ⁴⁴Ti mass can be used to constrain supernova core-collapse dynamics and nucleosynthesis. The amount of ⁴⁴Ti produced in a core-collapse supernova depends on the mass cut (how much mass falls back onto the neutron star), the

pre-supernova composition inside $2 M_\odot$, and the maximum temperature and density reached during the passage of the shock wave in the ejecta (Woosley & Hoffman 1991; Thielemann, Hashimoto, & Nomoto 1990). There are large uncertainties in these parameters, which would be greatly constrained by measurements of ⁴⁴Ti. To γ -ray observers, the amount of ⁴⁴Ti mass detected by COMPTEL means possible detections of ⁴⁴Ti-line hot spots from other nearby and recent supernova remnants.

In this paper, OSSE adds the excitement of a detection of hard X-rays between 40-200 keV from Cas A. X-rays above 30 keV have been anticipated by HEAO A-2 data (Pravdo & Smith 1979), which suggested that thermal bremsstrahlung emission of $kT \sim 30 \text{ keV}$ was needed, in addition to an 8.6 keV component, to fit those data. The higher temperature component is interpreted as the emission from shocked circumstellar material (CSM) by the primary blastwave of the supernova and the lower temperature component is the emission from the reverse shocked ejecta. The model is supported by X-ray images from the the Einstein Observatory (Fabian et al. 1980), which show emission from two thin concentric shells with temperatures of 0.65 keV and 4 keV. The lower temperature is confirmed by ROSAT observation in the range 0.1–2.4 keV whose emission can be fitted with $kT=0.68 \text{ keV}$ (Hartmann et al. 1995). However, the 2–12 keV *Tenma* data (Tsunemi et al. 1995) could be fitted with a single thermal bremsstrahlung continuum with temperature of 3.8 keV. EXOSAT 0.5 – 25 keV data (Jansen et al. 1988) do not require the $\sim 30 \text{ keV}$ thermal bremsstrahlung emission indicated by HEAO A-2 data, but it can not exclude that component. Jansen et al. (1988) concluded from EXOSAT images that the 3.8 keV component measured by *Tenma* is not the emission from the reverse-shocked ejecta but from the primary shocked CSM.

Another interpretation of Cas A emission above 16 keV has been proposed by Asvarov et al. (1989). They suggest that the hard X-ray spectrum is due to the bremsstrahlung

Report Documentation Page

Form Approved
OMB No. 0704-0188

Public reporting burden for the collection of information is estimated to average 1 hour per response, including the time for reviewing instructions, searching existing data sources, gathering and maintaining the data needed, and completing and reviewing the collection of information. Send comments regarding this burden estimate or any other aspect of this collection of information, including suggestions for reducing this burden, to Washington Headquarters Services, Directorate for Information Operations and Reports, 1215 Jefferson Davis Highway, Suite 1204, Arlington VA 22202-4302. Respondents should be aware that notwithstanding any other provision of law, no person shall be subject to a penalty for failing to comply with a collection of information if it does not display a currently valid OMB control number.

1. REPORT DATE 1996		2. REPORT TYPE		3. DATES COVERED 00-00-1996 to 00-00-1996	
4. TITLE AND SUBTITLE CGRO/OSSE observations of the Cassiopeia A SNR				5a. CONTRACT NUMBER	
				5b. GRANT NUMBER	
				5c. PROGRAM ELEMENT NUMBER	
6. AUTHOR(S)				5d. PROJECT NUMBER	
				5e. TASK NUMBER	
				5f. WORK UNIT NUMBER	
7. PERFORMING ORGANIZATION NAME(S) AND ADDRESS(ES) Naval Research Laboratory, E.O. Center for Space Research, 4555 Overlook Avenue, SW, Washington, DC, 20375				8. PERFORMING ORGANIZATION REPORT NUMBER	
9. SPONSORING/MONITORING AGENCY NAME(S) AND ADDRESS(ES)				10. SPONSOR/MONITOR'S ACRONYM(S)	
				11. SPONSOR/MONITOR'S REPORT NUMBER(S)	
12. DISTRIBUTION/AVAILABILITY STATEMENT Approved for public release; distribution unlimited					
13. SUPPLEMENTARY NOTES					
14. ABSTRACT					
15. SUBJECT TERMS					
16. SECURITY CLASSIFICATION OF:			17. LIMITATION OF ABSTRACT	18. NUMBER OF PAGES 4	19a. NAME OF RESPONSIBLE PERSON
a. REPORT unclassified	b. ABSTRACT unclassified	c. THIS PAGE unclassified			

from accelerated nonthermal electrons at shock fronts. It is this same electron distribution that produces the radio synchrotron from Cas A SNR which has a spectral index, $\alpha = 0.76$ (where $S_\nu \propto \nu^{-\alpha}$, Allakhverdiyev et al. 1986; Anderson et al. 1991). The model predicts a power-law X-ray spectrum with power index, $\delta = \alpha + 1.5 = 2.26$, above 16 keV, which is consistent with observations to date (Asvarov et al. 1989, The et al. 1995).

2. Observations

After the first OSSE Cas A observation (VP34) reported by The et al. (1995), we obtained three more observations. These OSSE pointing strategies were very similar to VP34. The duration and number of detectors in each viewing period are listed in Table 1. The OSSE spectral analysis technique subtracts background measured in offset pointings of the detectors from the source pointings (Johnson et al. 1993). The quadratically interpolated background estimates are subtracted from each source spectrum to obtain a difference spectrum for each 2-minute source pointing. The average spectrum of each of the four OSSE detectors is obtained for each viewing period. To fit the data, a single photon model is convolved with an instrument response function for each detector for each observation, and each resulting count rate model is compared with each observed count rate spectrum. A detailed description of OSSE performance and spectral data analysis procedures can be found in Johnson et al. (1993).

Table 1. Viewing Periods of OSSE Cas A Observations

VP#	Start Date	Stop Date	No. Det	Live Time (10^5 sec)
VP 34	92/198	92/219	4	6.0
VP 411.1	95/045	95/052	4	3.3
VP 419.5	95/129	95/143	2	3.1
VP 420	95/143	95/157	4	6.2
Total				18.6

3. X-ray Continuum Detection

Figure 1 shows the photon spectra measured by OSSE and by previous experiments. The dashed-dotted line is the best thermal bremsstrahlung fit to the OSSE spectrum between 0.04–0.25 MeV. The model parameters are shown in Table 2. The bremsstrahlung temperature $kT=35$ keV is in agreement with the higher temperature component suggested by HEAO A-2 observations (Pravdo & Smith 1979). The HEAO A-2 high-T component intensity is ($\sim 1.7 \times 10^{-10}$ ergs cm^{-2} s^{-1}) and its 3σ upper limit in the energy range of 0.2–60 keV is $\sim 2.6 \times 10^{-9}$ ergs cm^{-2} s^{-1} , while

the extrapolated flux of OSSE measurement in the same range of energy is $\sim 7.3 \times 10^{-11}$ ergs cm^{-2} s^{-1} .

The power-law spectrum proposed by Asvarov et al. (1989, Eq.(2) in The et al. 1995) fitted to OSSE data between 0.04–0.25 MeV does not produce a good fit ($\chi_\nu^2 = 1.183$ for D.O.F.= 488) shown in Figure 1 as a long-dashed line. If we allow the overall intensity parameter to vary the result improves to $\chi_\nu^2 = 1.138$ with intensity of $(10.7 \pm 2.4) \times 10^{-4}$ γ cm^{-2} s^{-1} MeV^{-1} at 0.1 MeV. If we relax both the power-law index and the intensity in the fit, we obtain the fit shown in Figure 1 as a solid line whose parameters are shown in Table 2.

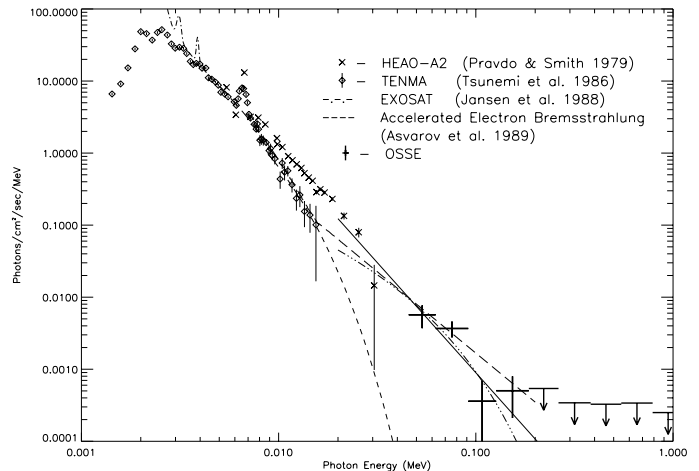


Fig. 1. Cas A broad-band photon spectrum. This figure shows data from all four OSSE observations. OSSE upper limits are 2σ . The detected continuum is consistent with the extrapolation of HEAO A-2 data and with the accelerated electron bremsstrahlung spectrum (long-dashed line) for energy above 16 keV. The solid line is the best-fit power-law and the dashed-dotted line is the best-fit thermal bremsstrahlung to the energy range 0.04 – 0.25 MeV. The short-dashed line is the bremsstrahlung fit to *Tenma* data given by Tsunemi et al. (1986).

In this measurement OSSE detects an X-ray continuum above 40 keV. This continuum is consistent with an extrapolation from HEAO A-2 data. Comparison of *Tenma* and OSSE data clearly shows that OSSE detects another hard component not detected previously. However, *Tenma* and HEAO A-2 data are not consistent with each other. A measurement of the entire 10–200 keV energy range is needed to clarify this situation.

4. ^{44}Ti γ -Line Fluxes

In searching for ^{44}Ti line emission from Cas A SNR, we perform an analysis similar to that of The et al. (1995, i.e., assuming line widths of 2.5% of line rest energies in fittings). Fit results are tabulated in Table 3 and shown in

Table 2. 40–250 keV Continuum Fluxes

Continuum	Flux ^a	power-law index or kT (keV)	χ^2_ν	D.O.F.	4σ Lower Limit ^b
Power Law	$(+8.95 \pm 2.11)$	$(-3.06 \pm_{0.41}^{0.44})$	1.136	486	+0.23
Exponential	$(+9.00 \pm 2.65)$	$(23.3 \pm_{3.9}^{5.1})$	1.134	486	+0.03
Therm. Brems.	$(+9.16 \pm_{2.54}^{2.47})$	$(35.0 \pm_{7.6}^{11.2})$	1.134	486	+0.04

^a Flux at 100 keV in units of $10^{-4} \gamma \text{ cm}^{-2} \text{ s}^{-1} \text{ MeV}^{-1}$.

^b 4σ lower-limit flux at 100 keV in units of $10^{-4} \gamma \text{ cm}^{-2} \text{ s}^{-1} \text{ MeV}^{-1}$.

Figures 2 and 3. We can not confirm the detection of the 1.157 MeV ^{44}Ti line by COMPTEL, however, our results are much more consistent with the lower COMPTEL line flux, $(4.2 \pm 0.9) \times 10^{-5} \gamma \text{ cm}^{-2} \text{ s}^{-1}$, reported in these proceedings (Schönfelder 1995) than with the initial report of $(7.0 \pm 1.7) \times 10^{-5} \gamma \text{ cm}^{-2} \text{ s}^{-1}$ (Iyudin 1994). This lower flux from all observations apparently results from the addition of new observations with quite low measured line flux. Considering statistical uncertainties only, the OSSE and COMPTEL measurement are now formally consistent with each other at 15% confidence, for a true flux value of $3.5 \times 10^{-5} \gamma \text{ cm}^{-2} \text{ sec}^{-1}$. This flux translates into $(1.0, 3.0) \times 10^{-4} M_\odot$ of ^{44}Ti for ^{44}Ti half-life of (66.6, 46.4) yrs respectively (Frekers et al. 1980; Alburger & Harbottle 1990), distance of 2.92 kpc (Braun 1985), and age of 314 yrs (Ashworth 1980). This ^{44}Ti mass perhaps suggests that the higher ^{44}Ti half-life is preferred as it is unusual to produce ^{44}Ti mass larger than $10^{-4} M_\odot$ in supernova models (Timmes et al. 1995).

5. Discussion

Early X-ray observations of Cas A by the Einstein Observatory, HEAO A-2, *Tenma*, and EXOSAT in general detected either a single or two-component thermal spectrum in the ranges 0.6–1 keV and 3.5–8 keV. The spectra were interpreted as emissions from two physical regions in the reverse shock model. Itoh (1994) and Hamilton (1983) in calculating X-ray emission from young SNRs interaction with CSM considered the nonequilibrium ionization and temperature relaxation between electrons and ions behind the shock. In the models where the electron and ion temperatures are not in equilibrium, the ratio of the electron temperature in the blastwave CSM and in the reverse shocked ejecta is $\gtrsim 1$. This model explains most data from previous experiments but not the higher temperatures suggested by OSSE data. However in the models where the electron and ion temperatures are equilibrated at the shock front, the electron temperature in the shocked CSM can be an order of magnitude larger than the electron temperature in the denser ejecta (~ 3.8 keV, Itoh 1994 and Hamilton 1983). Thus if the photons detected by OSSE are indeed of thermal origin, the electrons and ions in the shock fronts are in equilibrium (Fabian et al. 1980).

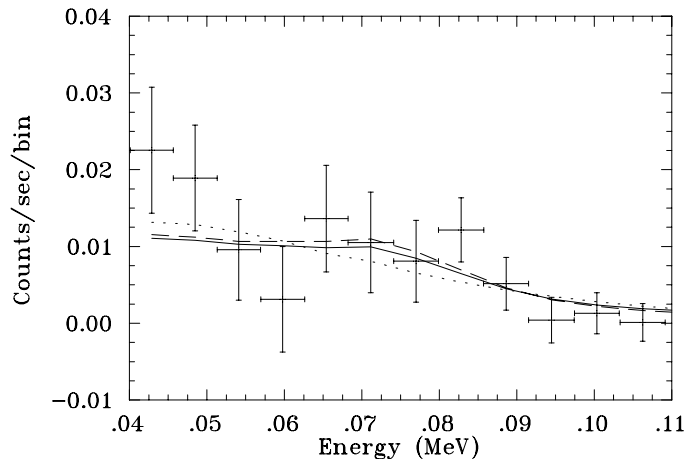


Fig. 2. Average OSSE count spectrum (four observations) from 0.04 to 0.11 MeV with fitted models overlaid. The solid line is the best simultaneous fit to the separate ranges 0.04–0.15 MeV and 0.8–1.5 MeV with independent continua and three ^{44}Ti decay γ -ray with fixed flux ratios of 1:0.98:1. The best-fit line amplitude is $(+1.76 \pm_{1.48}^{1.51}) \times 10^{-5} \gamma \text{ cm}^{-2} \text{ sec}^{-1}$. The dashed line is the best fit to the energy range of 0.04–0.15 MeV with an exponential continuum and the 68 and the 78 keV lines fitted simultaneously. The dotted line is the best fit of an exponential continuum only.

The total measured energy flux received from the shocked CSM is $\sim 9 \times 10^{-11} \text{ ergs cm}^{-2} \text{ sec}^{-1}$ and the total measured energy flux received from the reverse-shocked ejecta is $\sim 2 \times 10^{-9} \text{ ergs cm}^{-2} \text{ sec}^{-1}$.

Alternatively, the detected continuum can be interpreted as the emission from nonthermal, shock-accelerated electrons. This model is supported by the similarity in the morphology between X-ray images and radio maps of Cas A (Anderson et al. 1991)

6. Conclusions

- OSSE, with more data than was available in initial analyses (The et al. 1995), detects the 40–120 keV continuum flux from Cas A. The best power law fit to the continuum is $(+8.95 \pm 2.11) \times 10^{-4} (E/0.1 \text{ MeV})^{-(3.06 \pm_{0.44}^{0.41})} \gamma \text{ cm}^{-2} \text{ s}^{-1} \text{ MeV}^{-1}$. This power-

Table 3. Measured Cas A Line Fluxes

Source	Line Energy (keV)	Continuum (MeV)	Line Flux ^a	χ^2_ν	D.O.F.
⁴⁴ Ti	67.9 & 78.4 ^b	Exp. (0.04-0.15)	(+1.92 ± ^{1.55} _{1.50})	1.132	248
	1,157	Linear (0.80-1.50)	(-0.78 ± 2.50)	1.006	1552
	67.9, 78.4, & 1,157 ^c	Exp. & Linear (0.04–0.15 & 0.80–1.50)	(+1.76 ± ^{1.51} _{1.48})	1.014	1780

^a Flux in each line in units of $10^{-5} \gamma \text{ cm}^{-2} \text{ s}^{-1}$.

^b Simultaneous fit to 68 keV and 78 keV lines.

^c Setting the 68 keV, 78 keV, and 1.157 MeV line fluxes to ratios of 1 : 0.98 : 1.

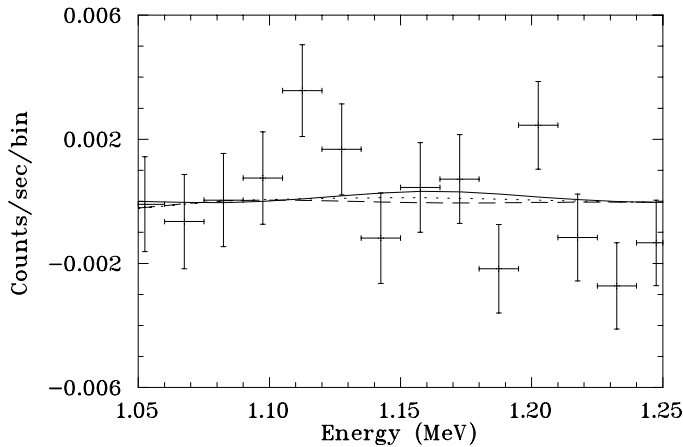


Fig. 3. Same as Figure 2 but for energy range 1.05–1.25 MeV. The dashed line is the best fit to the energy range of 0.8–1.5 MeV with a linear continuum and the 1.157 MeV ⁴⁴Ti line. The dotted line is a fit of a linear continuum only. (see Table 3 for parameters).

law continuum is consistent with emission from shock-accelerated electrons that produce the radio emission from Cas A (Asvarov et al. 1989).

- The detected continuum can be fit equally well with an exponential continuum or a thermal bremsstrahlung continuum. The thermal bremsstrahlung ($kT \approx 35$ keV) is identical to the second component needed to fit HEAO A-2 spectrum (Pravdo & Smith 1979) and can be interpreted as the emission from shocked CSM by the primary blastwave of the supernova.
- The best fit to three ⁴⁴Ti lines gives a ⁴⁴Ti line flux of $(1.76 \pm^{1.51}_{1.48}) \times 10^{-5} \gamma \text{ cm}^{-2} \text{ s}^{-1}$ for each line with a 99% confidence upper limit of $5.7 \times 10^{-5} \gamma \text{ cm}^{-2} \text{ s}^{-1}$. This measurement is consistent with zero flux, but is reasonably consistent with the 1.157 MeV flux measured by COMPTEL as reported in these proceedings $(4.2 \pm 0.9) \times 10^{-5} \gamma \text{ cm}^{-2} \text{ s}^{-1}$; Schönfelder 1995). Combining the new COMPTEL and OSSE ⁴⁴Ti line flux measurements, the most probable ⁴⁴Ti line flux is $3.5 \times 10^{-5} \gamma \text{ cm}^{-2} \text{ s}^{-1}$, which translates into $1.0 \times 10^{-4} M_\odot$. This mass is compatible with nu-

cleosynthesis calculations for ⁴⁴Ti half-life of 66 yrs, distance of 2.9 kpc, and age of 314 yrs.

Acknowledgements. We thank R. Diehl and A. Iyudin for very useful discussions on COMPTEL's results of Cas A observations. This research was supported by NASA DPR S-10987C.

References

- Alburger, D. E., & Harbottle, G. 1990, Phys. Rev. C, 41, 2320
- Allakhverdiyev, A. O., Asvarov, A. I., Guseinov, O. H., & Kasumov, F. K. 1986, Ap&SS, 123, 237
- Anderson, M., Rudnick, L., Leppik, P., Perley, R., & Braun, R. 1991, ApJ, 373, 146
- Ashworth, W. B. 1980, J. History Astron., 11, 1
- Asvarov, A. I., Guseinov, O. Kh., Dogel, V. A., & Kasumov, F. K. 1989, Soviet, Astron. 33, 532
- Braun, R. 1985, Ph.D. thesis, Leiden State Univ.
- Fabian, A. C., Willingale, R., Pye, J.P., Murray, S.S., & Fabiano, G. 1980, MNRAS, 193, 175
- Frekers, D., et al. 1983, Phys. Rev. C, 28, 1756
- Gull, S.F. 1975, MNRAS, 171, 263
- Hamilton, A. J. S., Sarazin, C. L., & Chevalier, R. A. 1983, ApJS, 51, 115
- Hartmann, D. H., et al. 1995, A&A, in preparation
- Itoh, H. 1977, PASJ, 29, 813
- Iyudin, A., et al. 1994, A&A, 284, L1
- Jansen, F., Smith, A., Bleeker, J. A. M., De Korte, P. A. J., Peacock, A., & White, N. E. 1988, ApJ, 331, 949
- Johnson, W. N., et al. 1993, ApJS, 86, 693
- Nomoto, K., Thielemann, F. K., & Yokoi, K. 1984, ApJ, 286, 644
- Pravdo, S. H., & Smith, B. W. 1979, ApJ, 234, L195
- Schönfelder, V., et al. 1995, these proceedings
- The, L.-S., et al. 1995, ApJ, 444, 244
- Timmes, F. X., Woosley, S. E., Hartmann, D. H., & Hoffman, R. D. 1995, ApJ, in press
- Tsunemi, H., Yamashita, K., Masai, K., Hayakawa, S., & Koyama, K. 1986, ApJ, 306, 248
- Woosley, S. E., & Hoffman, R. D. 1991, ApJ, 368, L31.